Local Features and Takagi-Sugeno Fuzzy Logic based Medical Image Segmentation

Umer JAVED[1], Muhammad Mohsin RIAZ[2], Abdul GHAFOOR[2], Tanveer Ahmed CHEEMA[1]

[1]School of Engineering and Applied Sciences, Isra University, Islamabad, Pakistan
[2]College of Signals, National University of Sciences and Technology (NUST), Islamabad, Pakistan

engr.umerjaved@gmail.com, mohsinriaz@mcs.edu.pk, abdulghafoor-mcs@nust.edu.pk, cheema@isra.edu.pk

Abstract. *This paper presents an improved region scalable fitting model that uses fuzzy weighted local features and active contour model for medical image segmentation. Local variance is used with local entropy to extract the regional information from the image which is then processed with the Takagi-Sugeno fuzzy system to compute weights. The use of regional descriptors enables this model to segment the inhomogeneous intensity images. The proposed objective function is minimized by using level set function. Performance evaluation of the proposed and existing model is achieved with the help of a probability rand index, global consistency error, the number of iterations and computation time taken. Extensive experiments on a series of real X-ray and MRI medical images shows the proposed technique offers better segmentation accuracy in lesser number of iterations and computation time.*

Keywords

Image segmentation, fuzzy logic, active contours.

1. Introduction

Image segmentation plays a vital role in several medical image analysis applications, including surgical planning and diagnosis. Numerous techniques have been introduced to achieve efficient and accurate medical image segmentation [1], [2]. Active contours are being extensively used in image segmentation. Earlier geometric active contours were built on the level sets and curve evolution. The surface evolution problem is frequently solved by using level set method [3]-[5]. The initial contour is represented as a zero level set of a higher dimensional level set [3]-[5]. Evolution of the contour is determined by solving the classic energy minimization problem. The basic principle is to evolve a curve, combined with constraints, to select a desired object. Active contours (for image segmentation) are categorized into edge-based [6], [7] and region-based [3], [5], [8] methods.

The edge based model uses image gradients to construct an edge stoping function that guides the contour towards desired object's boundary. Edge based methods are generally sensitive to image noise and the weak object boundaries [3], [9] and [10]. Such models may not work well in MRI images because of weak boundaries (due to low contrast ratio between grey and white matter) [10]. The region based models use region descriptors to guide contours and do not use image gradients. Therefore these models are less sensitive to initial conditions, weak boundaries and noise [10], [12].

Early region based models assume piecewise homogeneous intensities [3]-[5]. Such models fail to guide contours in intensity inhomogeneous images such as MRI images [12]. A classical active contour model, based on global information of an image, provides good results for images having smooth boundaries. It relies on piecewise homogenous intensities in regions [3]. However, its application towards MRI image segmentation is very limited because of complicated procedures involved and heterogenous regions [9], [11]. Recently the Region Scalable Fitting (RSF) energy model [9] (based on active contour and the variational level set) is used to address inhomogeneous intensities. This RSF model utilizes the intensity information of pixels located in the neighborhood defined by a scalable Gaussian kernel function. The model provides good result, however, it is prone to getting stuck in local minima [13] and is very sensitive to initialization of controlling parameters [11]. He et al. [13], combined local entropy and RSF model to overcome the above mentioned limitation. However, local entropy highlights edge information in the image, whereas inverse of local entropy can be used as region descriptor. Also, only local entropy is not a sufficient feature for obtaining accurate and efficient segmentation results in region based methods.

A scheme based on image local features (entropy and variance), in RSF model is proposed for medical image segmentation. Local variance is a region descriptor used for texture analysis [14]. Takagi Sugeno (TS) fuzzy is used to assign higher weights to pixels having less local entropy and variance, and vice versa. Qualitative and quantitative evaluations were carried out on medical image databases. The results show that the proposed scheme gives the improvement of medical image segmentation results in terms of accuracy and efficiency.
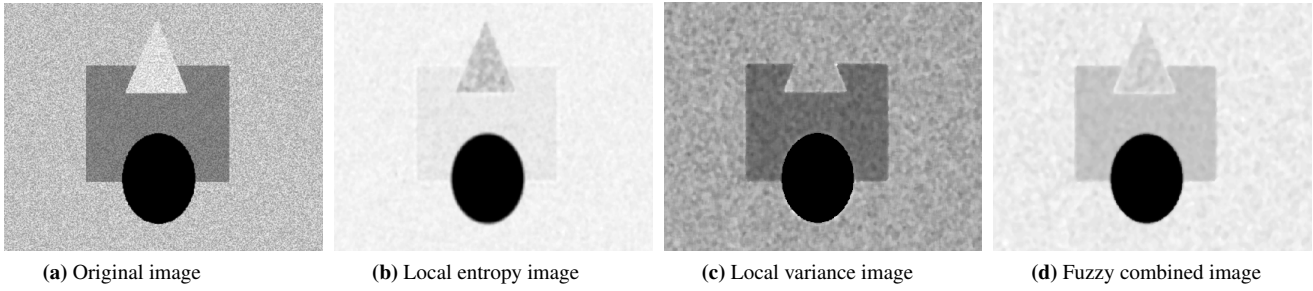
| **(a)** Original image | **(b)** Local entropy image | **(c)** Local variance image | **(d)** Fuzzy combined image |

Fig. 1. Different scenarios for evaluating features.

2. Preliminaries

Here a brief overview of the existing RSF model [9] is presented. Let C be a closed contour for the gray scale image I in domain Ω (divided into regions $\Omega_1 = inside(C)$ and $\Omega_2 = outside(C)$, λ_1 and λ_2 are positive constants [9], [13]. The Gaussian kernel function $K(u', v')$ (used to control the size of a local region), weighted average values $f_1(u, v)$ and $f_2(u, v)$ (used for an approximation of local image intensities in Ω_1 and Ω_2) are given as [9],

$$
\begin{aligned}
K(u', v') &= \left(\frac{1}{2\pi\rho^2}\right)\exp\left(\frac{-||u' - v'||^2}{2\rho^2}\right), \\
f_1(u, v) &= \frac{K(u, v) * [H_{\phi(u,v)}I(u, v)]}{K(u, v) * H_{\phi(u,v)}}, \\
f_2(u, v) &= \frac{K(u, v) * [(1 - H_{\phi(u,v)})I(u, v)]}{K(u, v) * (1 - H_{\phi(u,v)})}
\end{aligned}
\tag{1}
$$

where $\{m, n, u, v\} \in \Omega$, $u' = m - u$, $v' = n - v$, ρ is the standard deviation, $H_{\phi(u,v)}$ is the Heaviside function (used to determine the integrals inside and outside regions of contour) and $*$ denotes convolution operator. The smooth approximation of $H_{\phi(u,v)}$ and its derivative $\delta_{\phi(u,v)}$ are

$$
\begin{aligned}
H_{\phi(u,v)} &= \frac{1}{2}\left[1 + \frac{2}{\pi}\tan^{-1}\left(\frac{\phi(u, v)}{\varepsilon}\right)\right], \\
\delta_{\phi(u,v)} &= H'_{\phi(u,v)} = \frac{\varepsilon}{\pi(\varepsilon^2 + \phi^2(u, v))}
\end{aligned}
\tag{2}
$$

where ε indicates a constant value and ϕ is the level set function. The local entropy $L_E(u, v)$ is

$$
L_E(u, v) = -\frac{1}{u_1 \times v_1}\sum_{i_s}p(i_s)\log_2 p(i_s)
\tag{3}
$$

where $i_s \in [0, 1]$ are intensities in $u_1 \times v_1$ block of an image centered at (u, v) pixel and $p(i_s)$ represents the intensity histogram.

3. Proposed Fuzzy Active Contour

The weighted RSF model [13] assigns weight in proportion to the local entropy of each pixel. The use of local

entropy as a regional descriptor is not sufficient. A noisy image is shown in Fig. 1(a), results after applying local entropy are given in Fig. 1(b). It can be seen that local entropy overlooks the rectangular shaped region in the presence of noise. Results after applying local variance [14], [15] on the noisy image can be seen in Fig. 1(c). The image shows different values for local entropy and local variance due to presence of noise. This regional descriptor couldn't identify the triangular region. TS fuzzy logic is used to address this problem by combining the attributes of different features (i.e. local entropy and variance). Fig. 1(d) shows the effect of combining the attributes of local features by using TS fuzzy logic. The local variance $L_V(u, v)$ is defined as

$$
L_V(u, v) = \frac{1}{(2u_1 + 1)(2v_1 + 1)}\sum_{k=u-u_1}^{k=u+u_1}\sum_{l=v-v_1}^{l=v+v_1}(I(k, l) - \bar{I}(u, v))^2
\tag{4}
$$

where $\bar{I}(u, v)$ is the mean value of $u_1 \times v_1$ window centered at (u, v) pixel. The modified gradient flow of the proposed scheme is

$$
\begin{aligned}
\frac{\partial\phi(m, n)}{\partial t} = \delta_{\phi(m,n)}\Bigg[&\eta \, div\left(\frac{\nabla\phi(m, n)}{|\nabla\phi(m, n)|}\right) \\
&-\lambda_1\int_\Omega K(u', v')W_{EV}(u, v)|I(m, n) - f_1(u, v)|^2 du \, dv \\
&+\lambda_2\int_\Omega K(u', v')W_{EV}(u, v)|I(m, n) - f_2(u, v)|^2 du \, dv\Bigg] \\
&+\mu\left(\nabla\phi(m, n) - div\left(\frac{\nabla\phi(m, n)}{|\nabla\phi(m, n)|}\right)\right)
\end{aligned}
\tag{5}
$$

where W_{EV} are the weights calculated by TS fuzzy logic. Note that, for $W_{EV}(u, v) = 1$ and $W_{EV}(u, v) = L_E(u, v)$ the gradient flow in (5) reduces to the gradient flow given in [9] and [13], respectively.

In contrast to the Mamdani inference engine (where the output MFs are either linear or constant) [18], TS inference provides the flexibility to adjust output MFs using adaptive or optimization methods [19].

Let A^1, A^2 and A^3 (represent "High", "Medium" and "Low" respectively) be defined for L_E. The Gaussian MFs are

$$
\mu_{A^1}(x_1) = \exp\left(-\left(\frac{x_1 - \bar{x}_1^{(1)}}{\sigma_1^{(1)}}\right)^2\right),
$$

(a) 15 Iterations **(b)** 30 Iterations **(c)** 60 Iterations **(d)** 130 Iterations **(e)** 220 Iterations

(f) 15 Iterations **(g)** 30 Iterations **(h)** 60 Iterations **(i)** 130 Iterations
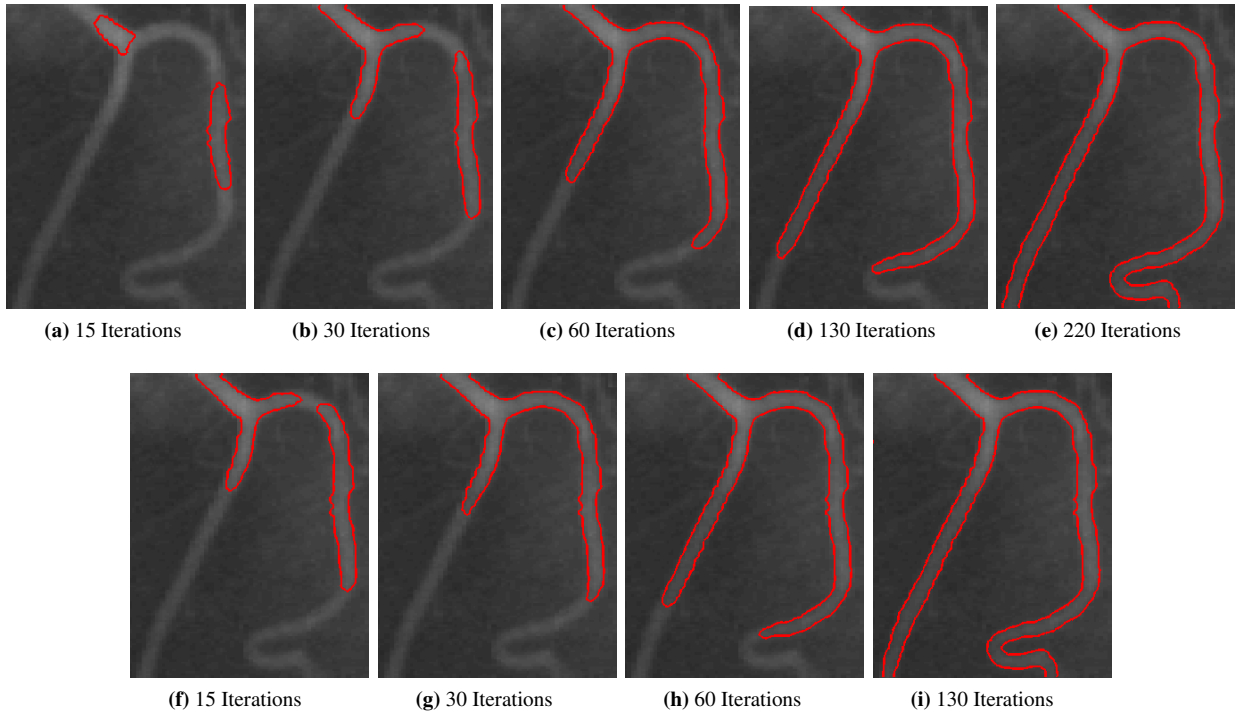
Fig. 2. Convergence analysis of algorithms (a)-(e) RSF model [9], (f)-(i) Proposed model.

$$\mu_{A^2}(x_1) = \exp\left(-\left(\frac{x_1 - \bar{x}_1^{(2)}}{\sigma_1^{(2)}}\right)^2\right)$$

and

$$\mu_{A^3}(x_1) = \exp\left(-\left(\frac{x_1 - \bar{x}_1^{(3)}}{\sigma_1^{(3)}}\right)^2\right).$$

Similarly, let B^1, B^2 and B^3 (represent "High", "Medium" and "Low" respectively) be defined for L_V. The Gaussian MFs are

$$\mu_{B^1}(x_2) = \exp\left(-\left(\frac{x_2 - \bar{x}_2^{(1)}}{\sigma_2^{(1)}}\right)^2\right),$$

$$\mu_{B^2}(x_2) = \exp\left(-\left(\frac{x_2 - \bar{x}_2^{(2)}}{\sigma_2^{(2)}}\right)^2\right)$$

and

$$\mu_{B^3}(x_2) = \exp\left(-\left(\frac{x_2 - \bar{x}_2^{(3)}}{\sigma_2^{(3)}}\right)^2\right)$$

where $\{x_1, x_2\} \in [0, 1]$. The means $\bar{x}_1^{(i_1)}$, $\bar{x}_2^{(i_2)}$ and variances $\sigma_1^{(i_1)}$, $\sigma_2^{(i_2)}$ (for $\{i_1, i_2\} \in \{1, 2, 3\}$) of fuzzy sets are calculated using K-means algorithm [16]. L_E is clustered into three classes based on histogram (similar procedure is adopted for L_V). The means and variances of each cluster are used as centers $\bar{x}_1^{(i_1)}$, $\bar{x}_2^{(i_2)}$ and spreads $\sigma_1^{(i_1)}$, $\sigma_2^{(i_2)}$ of MFs respectively.

The TS rule base for computing weights is:

IF $L_E(u, v)$ is $A^{(i_1)}$ AND $L_V(u, v)$ is $B^{(i_2)}$ THEN

$$z^{(i_1 + i_2 - 1)}(u, v) = \left(\frac{1}{1 + e^{-\eta_1 L_E(u,v)} + e^{-\eta_2 L_V(u,v)}}\right)^{i_1 + i_2 - 1}$$

where η_1 and η_2 are constants used to control the contribution of $L_E(u, v)$ and $L_V(u, v)$. Note that when $\eta_1 < \eta_2$, the effect of $L_V(u, v)$ is dominant compared to $L_E(u, v)$ on weights (and vice versa). Further note that large $i_1 + i_2$ reduces the output of rule-base (weight) which is desirable. The aggregated weights are

$$W_{EV}(u, v) = \frac{\sum\limits_{i_1=1}^{3}\sum\limits_{i_2=1}^{3} z^{(i_1+i_2-1)} t\{\mu_{A^{i_1}}(L_E), \mu_{B^{i_2}}(L_V)\}}{\sum\limits_{i_1=1}^{3}\sum\limits_{i_2=1}^{3} t\{\mu_{A^{i_1}}(L_E), \mu_{B^{i_2}}(L_V)\}} \quad (6)$$

where t represents the intersection operator and is chosen here as an algebraic product.

4. Results and Discussion

The results of proposed and existing RSF model are compared by using the Probability Rand Index (PRI) and Global Consistency Error (GCE). This comparison is carried out for quantifying the consistency of simulation results by taking into account the pairwise label relationship. Let G represent the ground truth image and G_{test} be the segmentation result. The PRI is defined as
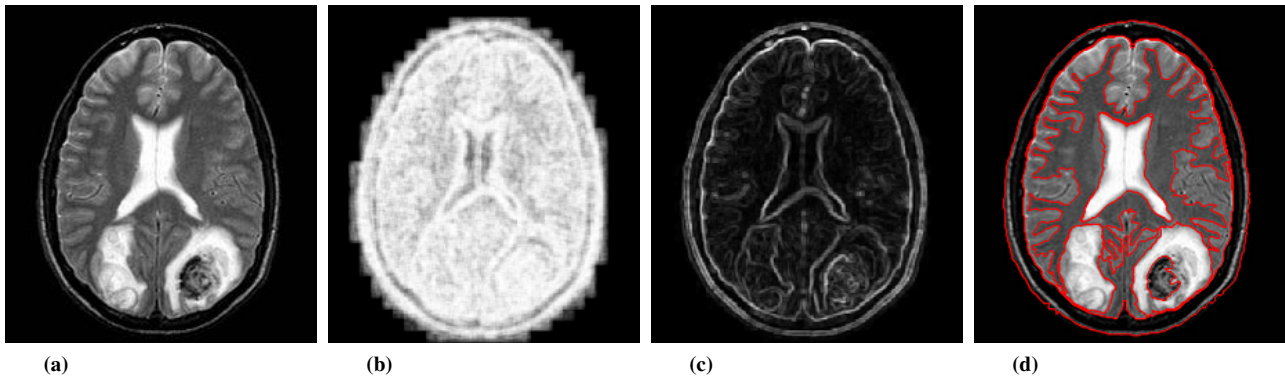
Fig. 3. Segmentation result for brain MRI (a) original image, (b) local entropy image, (c) local variation image and (d) segmentation by proposed technique.

Fig. 4. Segmentation result for brain MRI (a) original image, (b) local entropy image, (c) local variation image and (d) segmentation by proposed technique.
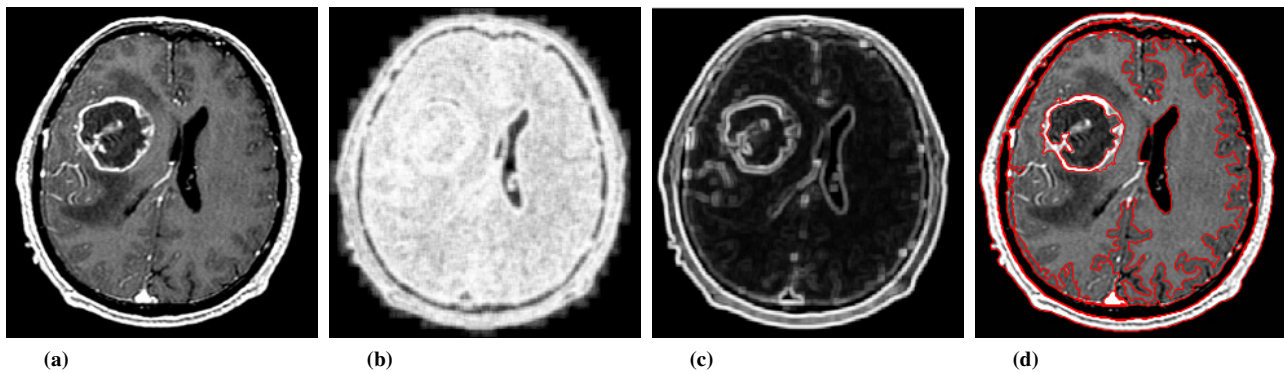
$$PRI(G_{test}, G) = \frac{2}{M(M-1)} \sum_{a,b} [\alpha_{a,b}\beta_{a,b} + (1-\alpha_{a,b})(1-\beta_{a,b})]$$

(7)

where $a \neq b$ and $M(M-1)$ denotes the possible unique pixel pairs out of total M data points. $\alpha_{a,b}$ represents the case when same labels exist in G_{test} and $\beta_{a,b}$ is the probability of having the same labels across G. The function shows the similarity between G_{test} and G. $PRI \in [0,1]$ with 0 and 1 representing no similarity and total similarity, respectively.

Another evaluation measure GCE is utilized for evaluating the consistency between image segmentations. Let $\xi(G_{test}, \zeta)$ and $\xi(G, \zeta)$ be the sets of pixels belonging to segment G_{test} and G, respectively. GCE is used to combine the values for the entire image in terms of an error measure, and is defined as

$$GCE(G_{test}, G) = \frac{1}{M} \min$$
$$\left\{ \frac{|\xi(G_{test}, \zeta) \cap \xi(G, \zeta)|}{|\xi(G_{test}, \zeta)|}, \frac{|\xi(G, \zeta) \cap \xi(G_{test}, \zeta)|}{|\xi(G, \zeta)|} \right\}.$$

(8)

This measure is tolerant of refinement and works for segmentations being compared with the similar number of segments. The range of GCE lies in between 0 and 1, where 0 indicates perfect image segmentation.

The proposed technique is implemented in Matlab (7.13, Release 2011b) and experiments were carried out on a Dell Inspiron, Intel Core i5 CPU, 2.1 GHz Processor, 4 GB ram. The results of existing and proposed schemes are analyzed on 15 X-ray blood vessels [9], [13] and 86 MRI real medical images. The accuracy of these results is compared with manual segmentation results similar to [22]-[24]. MRI datasets contains T1 and T2-weighted brain images from Harvard Medical School [20] and National Center for Biotechnology Information [21]. The parameters used during experiments are given in Tab. 1, η is initialized as $0.001 \times (255)^2$ [9], unless otherwise specified. For images which contain higher intensity inhomogeneities, small kernel size is preferable and vice versa.

Parameters	λ_1	λ_2	μ	κ	ρ	Δt	$u_1 \times v_1$
Values	1	1	1	2	3	0.1	3×3

Tab. 1. Simulation parameters.

In Fig. 2, the performance comparison of the existing RSF (Fig. 2(a - e)) and proposed scheme (Fig. 2(f - i)) for segmenting the X-ray blood vessel image is shown. Each image has a spatial resolution of 103×131. The final seg-
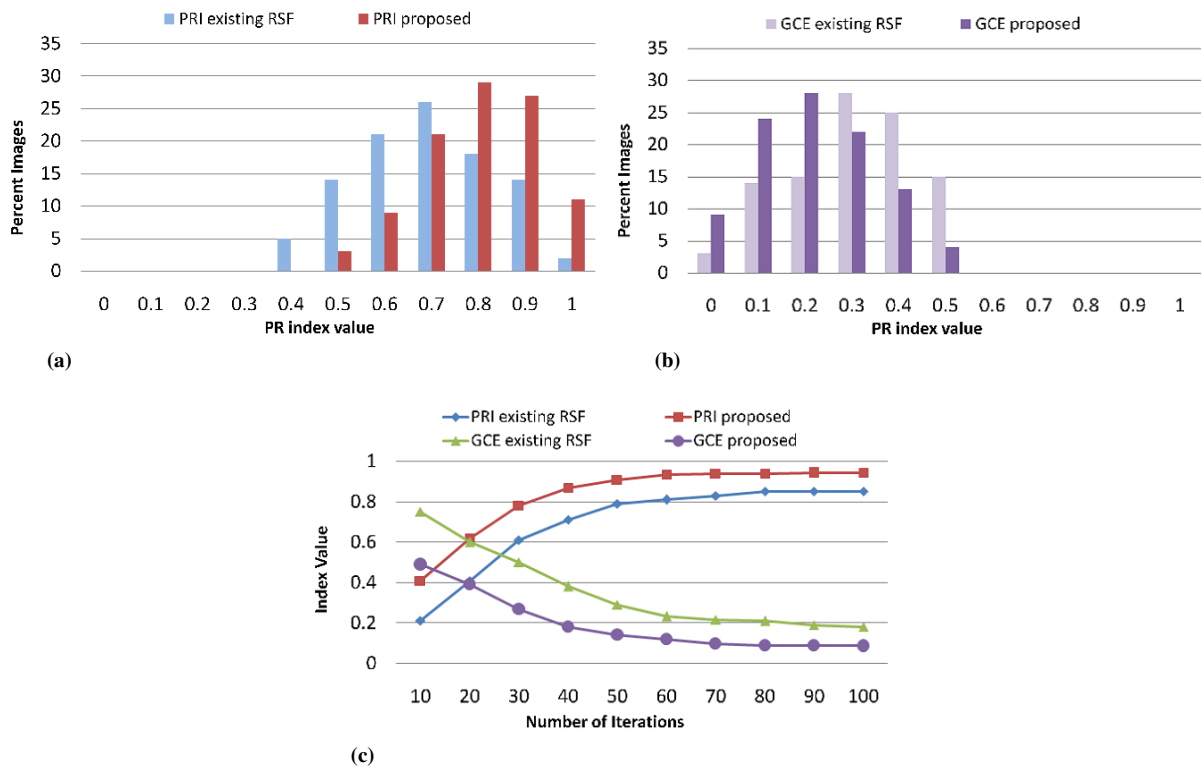
Fig. 5. PRI and GCE graphs for existing RSF model and proposed technique: (a) PRI distribution of percent images, (b) GCE distribution of percent images and (c) PRI and GCE values.

mentation results of the proposed method and weighted RSF model are shown in Fig. 2(e) and Fig. 2(i), respectively. Blood vessel boundaries are very weak in most of the image. This increases the difficulty of segmenting the vessel from the background. The results show that despite weak vessel boundaries in an original image, the proposed scheme provide faster convergence and gives more accurate segmentation results than the existing RSF model [9].

The segmentation result for T1 weighted brain MRI image containing a primitive neuroepithelial tumor of 256×256 resolution, is shown in Fig. 3. η is set as 0.04×255^2 whereas λ_1 and λ_2 are initialized as 1.0 and 2.0, respectively. The output of local entropy and variance is given in Fig. 3(b) and Fig. 3(c), respectively. Medical images have intensity inhomogeneity due to which the segmentation of all the objects becomes a non trivial task. The proposed technique has successfully segmented the objects present inside an image in 45 iterations, shown in Fig. 3(d). This illustrates the advantage of the proposed model, its ability to handle weak boundaries, complex background and intensity inhomogeneity.

A right frontal glioblastoma in T1 weighted brain MRI image is given in Fig. 4. The output of local entropy and variance is given in Fig. 4(b) and Fig. 4(c), respectively. In Fig. 4(d), the final segmentation of the proposed method is shown. This technique has successfully segmented the objects present inside the image in 55 iterations. This indicates

that by assigning weights, based on L_E and L_V, the proposed scheme performs accurate segmentation.

For quantitative analysis, the results of the proposed and existing RSF models are shown by using a Probability Rand Index (PRI) and Global Consistency Error (GCE) [17]. Fig. 5 shows the PRI and GCE graphs for 45 different images. These images belong to the above mentioned reputable medical image databases. Fig. 5(a) and Fig. 5(b) use percent images for computing PRI and GCE respectively. Note that PRI lies between 0.8 and 0.9 for most of the images using the proposed technique whereas for existing RSF model, PRI lies between 0.5 and 0.7. The GCE lies between 0.1 and 0.2 for most of the images using the proposed technique whereas for existing RSF model, GCE lies between 0.2 and 0.4. In Fig. 5(c), results are plotted for 100 iterations, since proposed technique, (in general), successfully segmented the ROI within these iterations. Note that soon after 70 iterations our proposed technique show no further improvement in PRI and GCE values. This indicates that the algorithm has reached its desired segmentation result. On the other hand RSF model keeps on converging even after 70 iterations. After several experiments the behavior shows that existing RSF model converges to proposed model's PRI and GCE values but after more iterations.

The average convergence analysis of existing RSF and proposed model, for blood vessel and brain images is given in Tab. 2. The spatial resolution of all images is also listed.

Techniques	Images	RSF	Proposed
Blood vessel	Iterations	220	130
	Computation time	8.58	5.15
Brain	Iterations	150	85
	Computation time	34.19	20.37

Tab. 2. Iterations and CPU time (in seconds) by RSF and proposed model.

The maximum iteration value for an experiment is achieved when the difference between two consecutive PRI samples is less than an arbitrary number τ. The suitable value of τ is based upon error tolerance criteria. The value of τ is initialized as 0.05 for experiments. Note that proposed method converges to desired result much faster then the existing RSF model. Our proposed model also offers lesser number of iterations than the existing technique. This indicates that assigning fuzzy weights to local descriptors not only reduces the computation time but converges faster than the standard RSF model.

5. Conclusion

This paper presents an improved RSF model that uses fuzzy weighted local features and active contour model for medical image segmentation. Local variance is used with local entropy to extract the regional information from the image which is then processed with the TS fuzzy system to compute weights. Higher weights are assigned to pixels having less local entropy and less local variance, and vice versa. The use of regional descriptors enables this model to segment the inhomogeneous intensity images. The proposed objective function is minimized by using level set function. Several experiments are conducted on real blood vessel and MRI brain images. The extensive experiments show the proposed technique offers better PRI and GCE values in lesser number of iterations and computation time.

References

[1] TRUC, P., KIM, T., LEE, S., LEE, Y. Homogeneity and density distance-driven active contours for medical image segmentation. *Computers in Biology and Medicine*, 2011, vol. 41, p. 292 - 301.

[2] LI, C., HUANG, R., DING, Z., GATENBY, J., METAXAS, D. A level set method for image segmentation in the presence of intensity inhomogeneities with application to MRI. *IEEE Transactions on Image Processing*, 2011, vol. 20, no. 7, p. 2007 - 2016.

[3] CHAN, T., VESE, L. Active contours without edges. *IEEE Transactions on Image Processing*, 2001, vol. 10, no. 2, p. 266 - 277.

[4] PARAGIOS, N., DERICHE, R. Geodesic active regions and level set methods for supervised texture segmentation. *International Journal on Computer Vision*, 2002, vol. 46, no. 3, p. 223 - 247.

[5] VESE, L., CHAN, T. A multiphase level set framework for image segmentation using the Mumford and Shah model. *International Journal on Computer Vision*, 2002 vol. 50, no. 3, p. 271 - 293.

[6] CASELLES, V., KIMMEL, R., SAPIRO, G. Geodesic active contours. *International Journal on Computer Vision*, 1997, vol. 22, no. 1, p. 61 - 79.

[7] PARAGIOS, N. K. *Geodesic active regions and level set methods: Contributions and applications in artificial vision PhD thesis*. Nice (France): University of Nice Sophia Antipolis, 2000.

[8] RONFARD, R. Region-based strategies for active contour models. *International Journal of Computer Vision*, 1994, vol. 13, no. 2, p. 229 - 251.

[9] LI, C., KAO, C., GORE, J. C., DING, Z. Minimization of region-scalable fitting energy for image segmentation. *IEEE Transactions on Image Processing*, 2008, vol. 17, no. 10, p. 1940 - 1949.

[10] WANG, Y., XIANG, S., PAN, C., WANG, L., MENG, G. Level set evolution with locally linear classification for image segmentation. *Pattern Recognition*, 2013, vol. 46, no. 6, p. 1734 - 1746.

[11] ZHENG, Q., ZHENTAI, L., YANG, W., ZHANG, M., FENG, Q., CHEN, W. A robust medical image segmentation method using KL distance and local neighborhood information. *Computers in Biology and Medicine*, 2013, vol. 43, no. 5, p. 459 - 470.

[12] WANG, L., LI, C., SUN, Q., XIA, D., KAO, C. Active contours driven by local and global intensity fitting energy with application to brain MR image segmentation. *Computerized Medical Imaging and Graphics*, 2009, vol. 33, no. 7, p. 520 - 531.

[13] HE, C., WANG, Y., CHEN, Q. Active contours driven by weighted region-scalable fitting energy based on local entropy. *Signal Processing Journal*, 2012, vol. 92, p. 587 - 600.

[14] DAROLTI, C., MERTINS, A., BODENSTEINER, C., HOFMANN, U. Local region descriptors for active contours evolution. *IEEE Transactions on Image Processing*, 2008, vol. 17, no. 12, p. 2275 - 2288.

[15] CHANG, D., WU, W., Image contrast enhancement based on a histogram transformation of local standard deviation, *IEEE Transactions on Medical Imaging*, 1998, vol. 17, no. 4, p. 518 - 531.

[16] WANG, L. X. *A Course in Fuzzy Systems and Control*. Upper Saddle River (NJ, USA): Prentice Hall, 1997.

[17] UNNIKRISHNAN, R., PANTOFARU, C., HEBERT, M. A measure for objective evaluation of image segmentation algorithms. In *IEEE Computer Society Conference on Computer Vision and Patten Recognition*. San Diego (CA, USA), 2005.

[18] YAGER, R., FILEV, D. *Essentials of Fuzzy Modeling and Control*. New York (USA): Wiley, 1994.

[19] TAKAGI, T., SUGENO, M. Fuzzy identification of systems and its applications to modeling and control. *IEEE Transactions on Systems, Man and Cybernetics*, 1985, vol. 15, no. 1, p. 116 - 132.

[20] *Harvard Medical Atlas Database*. [Online] Available at: http://www.med.harvard.edu/AANLIB/home.html .

[21] *National Center for Biotechnology Information*. [Online] Available at: http://www.ncbi.nlm.nih.gov/ .

[22] WEISENFELD, N. I., WARFIELD, S. K. Automatic segmentation of newborn brain MRI. *Neuro Image*, 2009, vol. 47, no. 2, p. 564 - 572.

[23] PRASTAWA, M., GILMORE, J. H., GERIG, G. Automatic segmentation of MR images of the developing newborn brain. *Medical Image Analysis*, 2005, vol. 9, no. 5, p. 457 - 466.

[24] KAUS, M. R., WARFIELD, S. K., NABAVI, A., BLACK, P. M., JOLESZ, F. A., KIKINIS, R. Automated segmentation of brain tumors. *Radiology*, 2001, vol. 218, no. 2, p. 586 - 591.

About Authors . . .

Umer JAVED received the BS and MS (Electronic Engineering) in 2007 and 2009, respectively. He is currently pursuing PhD in Electronic Engineering from Isra University, Pakistan. His research interests include fuzzy logic, neural networks and evolutionary computing.

Muhammad Mohsin RIAZ has completed PhD (Electrical Engineering) in 2013 from National University of Sciences and Technology (NUST), Pakistan. His research interests include signal processing, fuzzy logic, neural networks and evolutionary computing.

Abdul GHAFOOR completed his BE in 1994, MS in 2003 and PhD in 2007. Since 2008, he is with the Department of Electrical Engineering, College of Signals, National University of Sciences and Technology, Pakistan. His research interests include Control, Communication and Signal Processing. He has contributed over 100 research publications which include 40 papers in well reputed international journals.

Tanveer Ahmed CHEEMA received his PhD (Electronic Engineering) from Muhammad Ali Jinnah University, Pakistan in 2005. He is currently Associate Professor in Department of Electronic Engineering, Isra University, Pakistan. His research interests include image processing, template matching and neural networks.